



## A deterministic geometric representation of temporal rainfall: sensitivity analysis for a storm in Boston

N. Obregón<sup>a</sup>, B. Sivakumar<sup>b</sup>, C.E. Puente<sup>b,\*</sup>

<sup>a</sup>*Department of Civil Engineering, Universidad Javeriana, Bogotá, Colombia*

<sup>b</sup>*Department of Land, Air & Water Resources, University of California, Davis, CA 95616, USA*

Received 11 September 2001; revised 5 August 2002; accepted 23 August 2002

### Abstract

In an earlier study, Puente and Obregón [Water Resour. Res. 32(1996)2825] reported on the usage of a deterministic fractal–multifractal (FM) methodology to faithfully describe an 8.3 h high-resolution rainfall time series in Boston, gathered every 15 s and made of 1990 points, as the derived distribution of a classical multifractal measure via a fractal interpolating function. This work further studies the robustness of the FM methodology via an exhaustive sensitivity analysis aimed at obtaining even better FM descriptions for the Boston storm. This is carried out by varying a host of pertinent attributes that include usage of: (a) alternative objective functions for the inverse problem based on cumulative distributions of the records and of their derivatives; (b) a genetic algorithm in order to find the best FM parameters; (c) fractal interpolating functions passing by 3, 4 and 5 points, considering all relevant parameter-combination cases separately; and (d) two scales of aggregation, i.e. records with 199 and 1990 bins. The analysis indicates that previous results may indeed be improved when cumulative distributions of the records, rather than the records themselves, are employed in the FM parameter search, especially for representations based on 4 and 5 interpolating points and at the highest data resolution.

© 2002 Elsevier Science B.V. All rights reserved.

**Keywords:** Rainfall; Modeling; Fractals; Multifractals; Sensitivity analysis; Chaos

### 1. Introduction

Modeling the structure of temporal rainfall has been one of the most important research areas in hydrology over the past several decades, resulting in a variety of sophisticated models. Most current models are based on either stochastic (time series) methods or combinations of physically based representations with stochastic methods. Although significant success has

been attained using these methods, the (stochastic) models possess an important limitation in that they are constructed to preserve only some relevant statistical attributes of the rainfall records, rather than their complete geometric structure. These models also do not consider the effects of small distortions as identified in chaotic studies (Rodríguez-Iturbe et al., 1989; Berndtsson et al., 1994; Puente and Obregón, 1996; Sivakumar et al., 1999, 2001).

Puente (1992, 1994) introduced a fractal–multifractal (FM) approach for modeling complex temporal or spatial sets, as produced by non-linear systems. The idea behind this methodology is to think of the intricate

\* Corresponding author. Fax: +1-530-752-5262.

E-mail addresses: cepuente@ucdavis.edu (C.E. Puente), nobregon@javercol.javeriana.edu.co (N. Obregón), sbellie@ucdavis.edu (B. Sivakumar).

natural patterns as derived distributions of simple multifractal measures via fractal interpolating functions. An important trait of the FM method is that it is entirely deterministic and, hence, does not require any statistical assumptions, such as stationarity or ergodicity or a minimal record length. The basis for developing such an approach is the fact that seemingly irregular behavior can indeed be the result of simple deterministic systems influenced by a few non-linear interdependent variables (Lorenz, 1963; Meneveau and Sreenivasan, 1987).

The FM approach was successfully employed by Puente and Obregón (1996) to model a high-resolution storm (every 15 s for about 8.3 h) observed in Boston on October 25, 1980 (Rodríguez-Iturbe et al., 1989). A detailed comparison of the real and FM fitted rainfall time series revealed that the geometric procedure not only captured the timing and size of the largest peak present in the records but also preserved the overall appearance of the set, including secondary peaks and small noisy fluctuations. Such FM representation was reached minimizing a weighted sum of squared differences between attributes of the real and FM outcomes of equal length, searching FM parameter space using in succession the multidimensional simplex method (Press et al., 1989), simulated annealing (Otten and van Ginneken, 1989), and sequential quadratic programming (Zhou and Tits, 1993).

The ‘optimal’ solution reported preserved, as explicitly accounted for in the objective function, a list of statistical attributes, as follows: (1) the first 10 central and modal moments of the records when seen from the time axis; (2) the first 10 central moments of the records when seen from the intensity axis; and (3) the mass exponents function of the data (e.g. its multiscaling signature, see Puente and Obregón (1996)). At the end, the FM representation also captured a host of attributes not explicitly accounted for in the optimization exercise, such as: (1) the higher-order moments along both the time and intensity axes; (2) the overall shape of the autocorrelation and histogram functions of the records; (3) the scaling properties present in the power spectrum of the records; and (4) the possibly chaotic nature of the set of observations, as customarily done in non-linear dynamics studies (Sivakumar et al., 1999, 2001).

The goal of the present study is to further study the robustness of the FM approach and, in particular, to investigate whether even better approximations for the Boston storm may be obtained. This is done by performing a sensitivity analysis that accounts for the way one may estimate the FM parameters. These results are of relevance in future applications of the FM approach, for the parameter estimation exercise is both time consuming and non-trivial. The organization of this article is as follows. In Section 2, the FM approach is reviewed. Then, the detailed sensitivity analysis for the Boston set and the results thus obtained are reported. The article ends with its conclusions.

## 2. The fractal–multifractal approach

Fig. 1 shows on its right hand side the Boston storm under consideration, and the best approximation reported earlier via the FM approach next to it, i.e.  $dy$  (Puente and Obregón, 1996). As is seen, such a set is constructed transforming a multinomial multifractal measure,  $dx$  (bottom left) (Feder, 1988), via a fractal interpolating function that passes by five points, as indicated by the solid dots,  $f$  (Barnsley, 1988). Mathematically,  $dy$  is defined employing a derived distributions approach, considering all relevant events in  $x$  and adding their contributions, i.e.  $dy(B) = dx\{x : f(x) \in B\}$ , for all Borel subsets  $B$  on  $y$ , and hence can be interpreted as a weighted projection of the function  $f$ , with the weights given by the parent measure  $dx$ .

For a given set of  $N + 1$  points in the plane  $\{(x_0, y_0), (x_1, y_1), \dots, (x_N, y_N)\}$ ;  $x_0 < x_1 < \dots < x_N$ , measures  $dx$  and  $dy$  may be calculated iterating a suitable set of  $N$  contractile affine mappings (according to an appropriate set of  $N$  weights  $p_n$ ) and counting over a desired number of bins (the resolution of the records to be fitted) over  $x$  and  $y$  (Puente, 1994). Such mappings have the specific form

$$w_n \begin{pmatrix} x \\ y \end{pmatrix} = \begin{pmatrix} a_n & 0 \\ c_n & d_n \end{pmatrix} \begin{pmatrix} x \\ y \end{pmatrix} + \begin{pmatrix} e_n \\ f_n \end{pmatrix}, \quad (1)$$

where  $a_n$ ,  $c_n$ ,  $e_n$ , and  $f_n$  are related to the interpolating points and the free scaling parameters  $d_n$ ,  $0 \leq |d_n| < 1$ ,

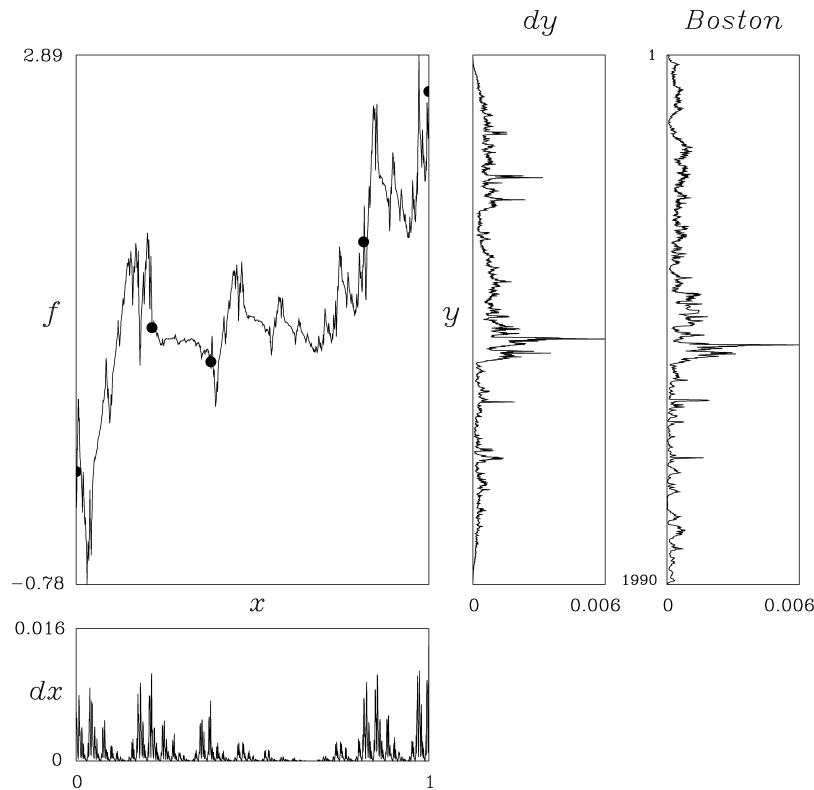


Fig. 1. The fractal-multifractal framework in two dimensions. A multifractal measure  $dx$  is transformed via a fractal interpolating function  $f$  into a derived measure  $dy$ . The set on the upper right corresponds to a storm in Boston.

via the conditions

$$w_n \begin{pmatrix} x_0 \\ y_0 \end{pmatrix} = \begin{pmatrix} x_{n-1} \\ y_{n-1} \end{pmatrix} \quad (2)$$

and

$$w_n \begin{pmatrix} x_N \\ y_N \end{pmatrix} = \begin{pmatrix} x_n \\ y_n \end{pmatrix} \quad (3)$$

for  $n = 1, 2, \dots, N$ . It turns out that the graph of a fractal interpolating function may be fractal, as its implied dimension  $Df$  is: (a) 1, if  $\sum |d_n| \leq 1$ , and (b)  $\geq 1$ , from  $\sum |d_n| d_n^{Df-1} = 1$ , if  $\sum |d_n| > 1$  (Barnsley, 1988). The FM representation shown in Fig. 1 is found iterating four affine mappings (according to four weights that yield the intermittencies of the parent measure) and hence is based on the 13 independent parameters (6 coordinates, 4 scalings, 3 independent iteration weights) included in the first

row of Table 1. That leads to a fractal interpolating function whose graph has a dimension of 1.51.

By varying the parameters of  $f$  and  $dx$ , i.e.  $(x_n, y_n)$ ,  $d_n$  and  $p_n$ , and by allowing projections to be found at directions other than  $y$ , i.e. at angles  $\theta$  other than  $180^\circ$ , a large variety of derived measures may be obtained. Overall, the following trends are found for the derived measures  $dy$  (Puente, 1994). When  $Df$  is close to one, they are typically multifractal and they have the desirable feature (as seen in Fig. 1) of being neither self-similar nor self-affine. As  $Df$  increases from 1 to 2, the measures become smooth and gradually acquire a density. In the limit, when  $Df$  tends to 2,  $dy$  becomes Gaussian, for every parent measure  $dx$  (Puente, 1992).

Given that multinomial multifractals have been found of relevance in the study of intermittent natural phenomena (Meneveau and Sreenivasan, 1987; Sreenivasan, 1991), the FM derived measures may be given a quasi-physical interpretation, i.e. they could be thought of as ‘projections’ of turbulence related

Table 1

Parameters for FM storms in Fig. 4. Values not shown below are set as follows:  $x_0 = 0$ ,  $y_0 = 0$ ,  $y_1 = 1$ , and  $x_N = 1$ , where  $N$  is the number of affine mappings

Storm	Coordinates						Projection angle $\theta$ (°)	
	$x_1$	$x_2$	$x_3$	$y_2$	$y_3$	$y_4$		
$dyV$ WRR96	0.215	0.382	0.815	0.763	1.596	2.756	180.0	
$dy * V$ WRR96	0.198	0.485	0.823	0.744	1.508	2.505	195.6	
$dy * V$	0.474	0.527	0.602	−6.250	8.644	−5.954	331.3	
$dy * IV$	0.322	0.826		1.125	2.585		59.0	
$dy * III$	0.492			−0.175			190.5	
	Scalings				Intermittencies			
	$d_1$	$d_2$	$d_3$	$d_4$	$p_1$	$p_2$	$p_3$	$p_4$
$dyV$ WRR96	−0.747	−0.082	0.482	0.744	0.331	0.161	0.135	0.374
$dy * V$ WRR96	−0.687	−0.032	0.416	0.764	0.348	0.142	0.142	0.368
$dy * V$	−0.052	0.328	0.401	−0.821	0.160	0.082	0.161	0.597
$dy * IV$	−0.889	0.235	−0.229		0.516	0.328	0.156	
$dy * III$	−0.954	−0.264			0.494	0.506		

phenomena. At the end, the FM approach interprets the (non-negative) data at hand (assumed herein to be noise free) as a normalized distribution, a probability measure, that is then encoded, as parsimoniously as possible, via a parent multifractal measure and a fractal interpolating function.

A relevant distinction between this approach and other state-of-the-art multifractal methods is that instead of concentrating on the statistics of the actual realization(s) (Lovejoy and Schertzer, 1990; Tessier et al., 1993), the FM methodology focuses on the whole geometry of the geophysical patterns, i.e. instead of concentrating on modeling or ‘characterizing’ the distribution of the data or relevant attributes, such as moments, the FM approach uses derived distributions to describe the data itself.

As there is no simple analytical formula that gives the derived measure,  $dy$ , nor its most common statistics, in terms of the FM parameters, the inverse problem for finding the best FM representation requires a numerical solution. As a result, this exercise becomes non-trivial due to: (1) the large number of combinations of parameters (coordinates, scalings, intermittencies and projection angle) that is 6, 10, and 14 for 3, 4, and 5 interpolating points (once  $x_0$ ,  $y_0$ ,  $y_1$ , and  $x_N$  are fixed); and (2) the practically infinite number of derived measures that may be generated, many of them sharing common statistical and multifractal features.

### 3. Sensitivity analysis for the Boston storm

As it has been our experience that the FM representations depend on a host of conditions (i.e. objective function, searching procedure, initial parameters, and data resolution) and as it has been our belief that even better FM descriptions could be obtained for the Boston storm, this section presents an exhaustive sensitivity analysis aimed at understanding the implied inverse problem better. To this effect, the analysis considers: (a) objective functions based on cumulative distributions of the records and their derivatives, that turn out to give better performance than the one used earlier based on moments and mass exponents (Puente and Obregón, 1996) or those based on the records themselves that lead to searches dominated by the largest peak in the storm; (b) FM representations calculated via a genetic algorithm (Duan et al., 1992) that improves the objective function faster than the optimization procedures used before (e.g. simulated annealing as in Fig. 1); (c) all possible sign combinations on the scalings  $d_n$  for 3, 4 and 5 interpolating points (i.e. leading to, in order, 4, 8, and 16 separate cases, see Eq. (1)) to avoid searches that travel from a quadrant to another and to more fully search the FM parameter space; and (d) two different scales (resolutions) for the records (199 and 1990 bins) to study if the faster calculations at

the aggregated scale, that lower the CPU search time from 3 days to less than one on a DEC 250 workstation, may be sufficient to model the actual records.

For reference, the attributes included in the optimization procedure (also included in the figures herein) are as follows:

- (a) Sum of square differences (over time) between cumulative distributions of the Boston and FM sets ( $\sum \Delta^2$ ).
- (b) Sum of square differences (over time) between cumulative distributions of normalized absolute one-lag derivatives of the Boston and FM sets ( $\sum \Delta^d$ ).
- (c) Sum of (a) and (b), that is  $\Delta = \sum \Delta^2 + \sum \Delta^d$ .

The following qualifiers, not explicitly considered during the optimization exercise, are also used to qualify the goodness of an optimal solution, as presented in the figures:

- (a) Maximum absolute difference (over time) between cumulative distributions of the Boston and FM sets ( $D$ ).
- (b) Distance from zero to the maximum of a normalized set ( $S$ ), i.e. the vertical scale of non-cumulative records.
- (c) Length from beginning to end of a cumulative distribution ( $L$ ), i.e. from (0, 0) to (1, 1) and belonging to the interval from square root of 2 to 2 that corresponds to uniform and multifractal measures, respectively.
- (d) Total range between a cumulative distribution and that of the uniform measure, that is  $R = |R^u| + |R^d|$ , where  $R^u$  and  $R^d$  are the respective maximum upper and lower differences between the distributions.

### 3.1. Results with 199 bins

Fig. 2 includes the best FM representations obtained using all sign combinations for 3 interpolating points, when the objective function is based on the cumulative distributions of the aggregated records (i.e.  $\sum \Delta^2$ ). As may be seen on the left, comparing individual frames with the first row containing the aggregated Boston set, the alternative scaling

combinations (i.e. cases c1–c4) result in various degrees of approximation (solid lines) of the data's cumulative distribution (in gray). Notice that, even though all cases give objective function values that may be considered 'small' (i.e. less than 0.166 in  $\sum \Delta^2$  as in case c1, as compared to typical starting values greater than 2), the alternative FM cases give rather poor 'storms' (all underestimating the peak magnitude as given by the quantity  $S$ ), indicating that using only the cumulative distribution of the records does not provide the desired improvements.

As seen on the right hand portion of Fig. 2, when the best FM parameters encountered at the 199 bin scale are used with the actual set of records in Boston (i.e. at the 1990 resolution), similarly poor trends are found. Notice that while cumulative distributions remain very similar, the FM storms vary from those aggregated at the left, for the smallest resolution typically results in more intermittent behavior (e.g. cases c2 and c4).

As the FM measures in Fig. 2 are either smoother than the original ones (i.e. cases c1, c3, and c4, as reflected by smaller values of  $L$  for both resolutions) or contain intermittencies not seen in the original sets (i.e. case c2), these results suggest that additional attributes, like the record's derivatives, ought to be included in the objective function. In this light, Fig. 3 shows what is found when the aforementioned exercise is repeated including in the objective function not only the cumulative distributions of the records but also those of their (normalized) absolute lag-one derivatives, i.e.  $\Delta = \sum \Delta^2 + \sum \Delta^d$ , as defined before.

As may be seen comparing the left hand portions of Figs. 2 and 3, although the additional attribute increases  $\sum \Delta^2$  (i.e. from 0.166 to 1.184, from 0.090 to 0.108, from 0.023 to 0.365, and from 0.023 to 0.145, for, in order, cases c1–c4), by improving the performance on the attribute  $\Delta$  (i.e. from 20.921 to 3.274, from 9.957 to 0.422, from 3.415 to 0.590, and from 2.602 to 1.156, for, in order, cases c1–c4) the new FM measures result in better overall fittings, that improve the magnitude of the largest peak (i.e. the attribute  $S$ ) and give close agreement on the quantity  $L$ , especially for cases c2 and c3.

As seen on the right hand portion of Fig. 3, when the best FM parameters minimizing  $\Delta$  at the 199 bin scale are used at the original resolution, the inherited FM storms exhibit, as in Fig. 2, more intermittency

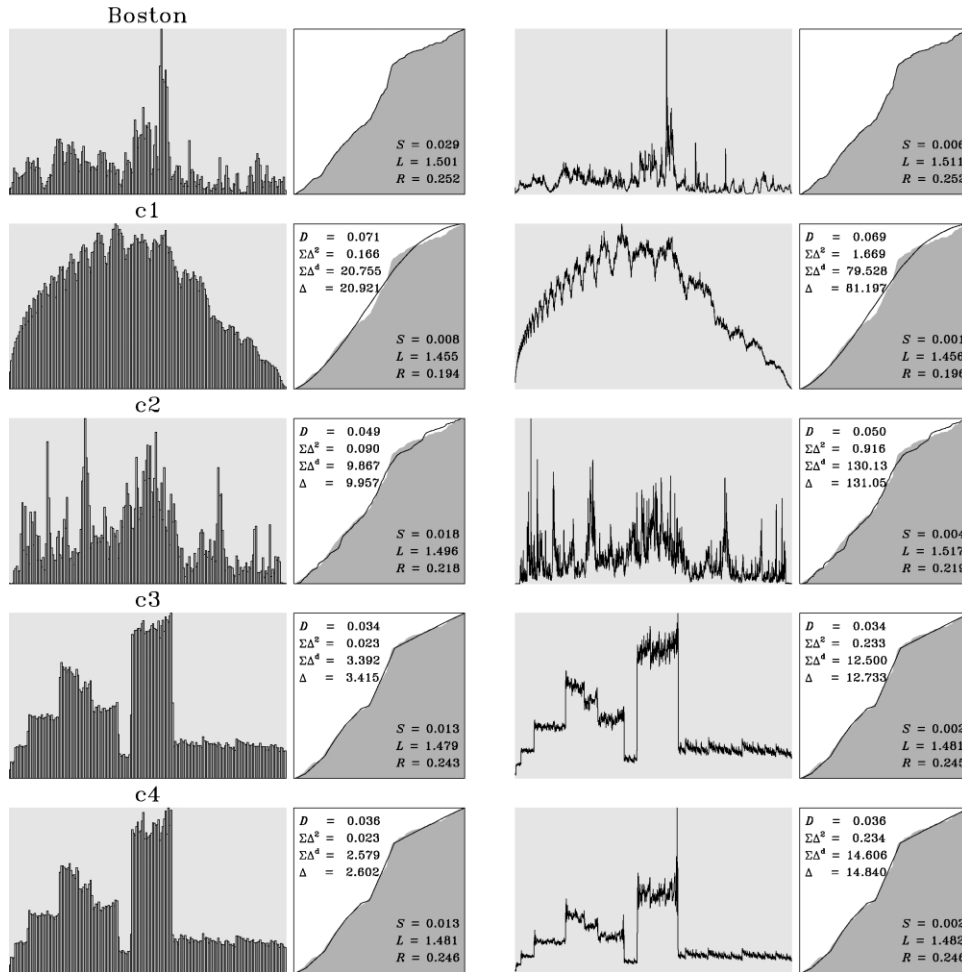


Fig. 2. Storms and cumulative distributions for 199 bins (left) and 1990 bins (right). The Boston records (top) are followed by FM fitted storms corresponding to sign combinations of scalings  $d_1$  and  $d_2$  for a fractal function that passes by 3 interpolating points, c1: + +, c2: + -, c3: - +, c4: - -.  $\Sigma\Delta^2$  is minimized at the 199 bin scale (see text for details).

than those at the 199 bin scale. This results in fittings that, while being worse in regards to  $\Sigma\Delta^2$  relative to the right hand side on Fig. 2, yield better overall representations. Notice how the major peak is better approximated for all storms, particularly in case c3 that, in a surprising manner, results in an increase in  $\Delta$  with respect to the same set in Fig. 2 (i.e. from 12.733 to 29.286). Observe how the best fit at the 199 bin scale, i.e. case c2, turns out not to be the best at the 1990 resolution, for two major spikes spring left and right of the real peak at such a scale.

Similar results to the ones shown here were also obtained for all sign combinations that correspond to

FM representations based on 4 and 5 interpolating points. Overall, the major trends of such optimization exercises (not shown) are similar to the ones just reported. As illustrated comparing Figs. 2 and 3, the usage of cumulative distributions of the records and their derivatives resulted in better FM fits than those found using just the cumulative distributions of the records, and good representations at the 199 bin scale did not necessarily translate into good fits at the 1990 resolution, due to the presence of additional intermittencies. At the end, those alternative representations captured, with varying degrees of success, the details present in the Boston storm,

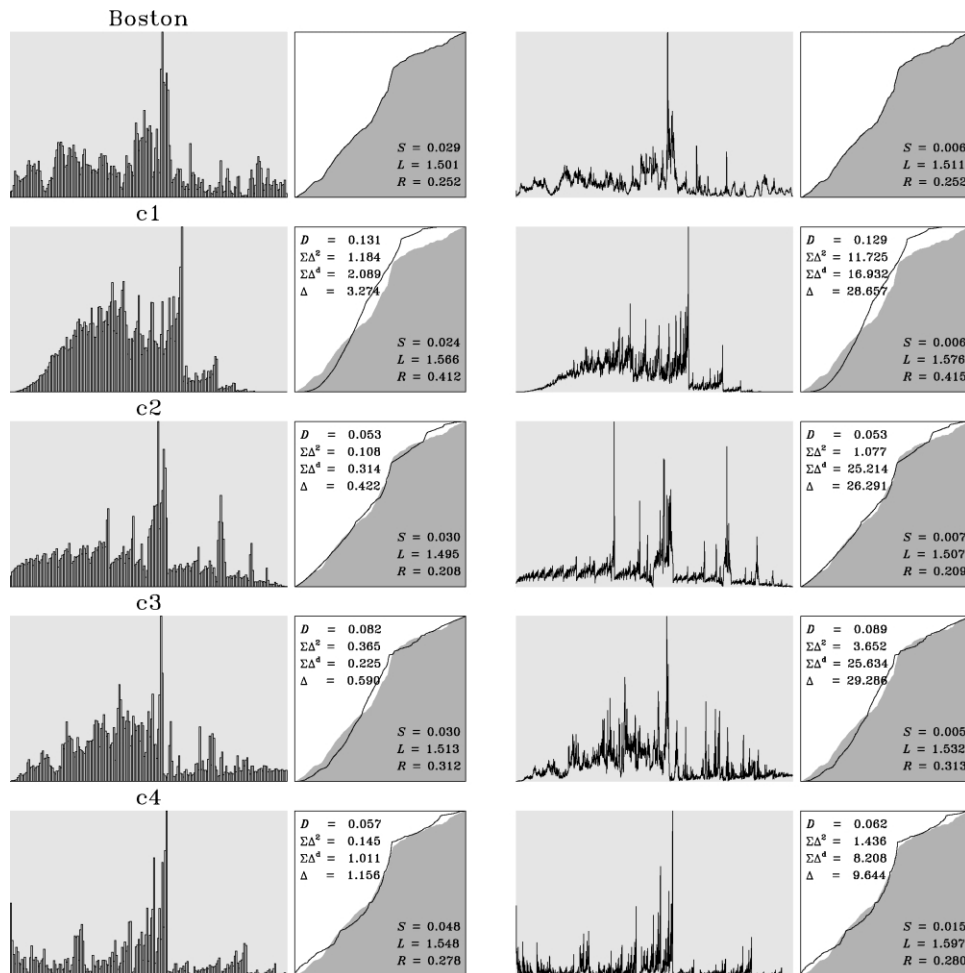


Fig. 3. Storms and cumulative distributions for 199 bins (left) and 1990 bins (right). The Boston records (top) are followed by FM fitted storms corresponding to sign combinations of scalings  $d_1$  and  $d_2$  for a fractal function that passes by 3 interpolating points, c1: + +, c2: + -, c3: - +, c4: - -.  $\Delta = \Sigma\Delta^2 + \Sigma\Delta^4$  is minimized at the 199 bin scale (see text for details).

and the addition of interpolating points typically resulted in improved behavior. For illustration, for the low resolution records (199 bin scale),  $\Delta$  took on values that ranged from 0.42 to 3.27 (left portion of Fig. 3), from 0.21 to 3.6, and from 0.21 to 1.32, for 3, 4, and 5 interpolating points, indicating that having more parameters yields, in general, better FM outcomes. The 'best' FM sets thus obtained, for 4 and 5 interpolating points (not shown), turned out to provide, for alternative cases with scalings on various quadrants, very good fits for the 199 bin Boston storm.

### 3.2. Results with 1990 data points

As good FM results from the lower resolution do not necessarily translate into good FM results at the higher resolution, this section presents what is found when the parameter search is repeated at the 1990 bin scale, minimizing  $\Delta$  starting the procedure at the best FM values encountered at the 199 resolution (i.e. the best sign combination case on the  $d_n$ 's), following a more computationally intensive search, that gives the optimal parameters included in Table 1. For comparison, Fig. 4 includes the following frames (from top



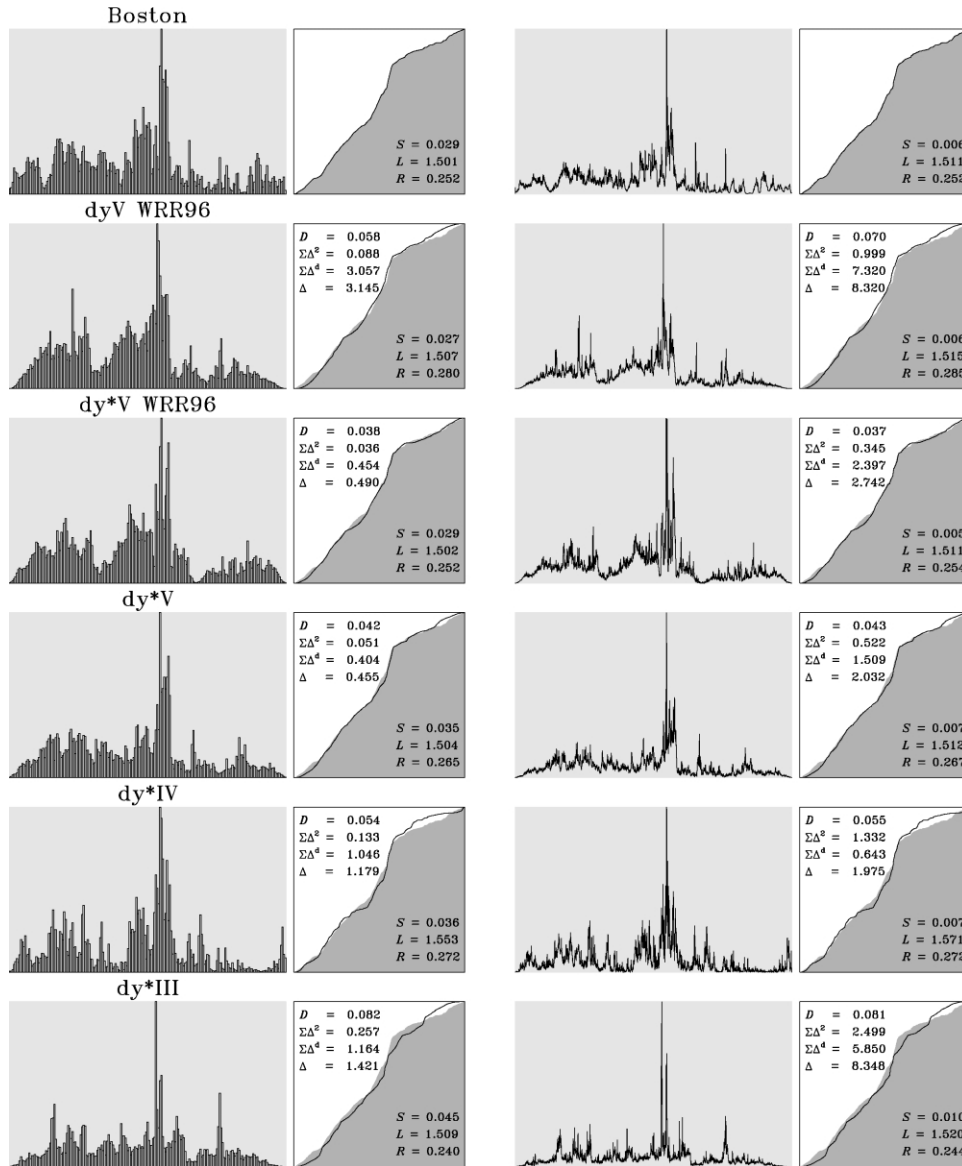


Fig. 4. Storms and cumulative distributions for 199 bins (left) and 1990 bins (right). From top to bottom: the Boston records, the best FM fit from moments and mass exponents (after Puente and Obregón (1996)) (dyV WRR96), the best FM representation obtained starting at the FM parameters of dyV WRR96 (dy\* V WRR96), and the best FM fits generated via fractal functions passing by 5, 4, and 3 interpolating points (dy\* V, dy\* IV, and dy\* III), starting with best parameters for the 199 bin scale.  $\Delta = \Sigma\Delta^2 + \Sigma\Delta^4$  is minimized at the 1990 bin scale (see text for details).

to bottom): (a) the Boston records at both resolutions; (b) the best FM fit via a fractal function passing by 5 points, as found via moments and mass exponents and as previously reported in Fig. 1 (dyV WRR96), i.e. Puente and Obregón (1996); (c) the best FM fit via

a fractal function passing by 5 points when dyV WRR96 parameters serve as a starting point in order to minimize  $\Delta$  via the genetic algorithm (dy\* V WRR96); and (d) in order, the best FM fits obtained starting at the best parameter values from the low



resolution exercise corresponding to fractal functions passing by 5 ( $dy^*V$ ), 4 ( $dy^*IV$ ), and 3 ( $dy^*III$ ) interpolating points.

As is seen, minimizing  $\Delta$  does result in improved approximations of the Boston storm, for such an attribute is lowered for all FM optimized measures on the right of Fig. 4: from 8.32 (Fig. 4,  $dy^*V$  WRR96) to 2.74 (Fig. 4,  $dy^*V$  WRR96); from 6.75 (not shown in a graph) to 2.03 (Fig. 4,  $dy^*V$ ); from 7.15 (not shown in a graph) to 1.97 (Fig. 4,  $dy^*IV$ ); and from 9.64 (Fig. 3, c4) to 8.35 (Fig. 4,  $dy^*III$ ). Clearly, the FM representations based on fractal functions passing by 4 or 5 interpolating points yield improved performance over the one based on 3 points, at both levels of aggregation. Notice that, while the FM storms corresponding to fractal functions interpolating 5 points lower the deviations in cumulative distributions ( $\sum \Delta^2$ ) relative to the results of Puente and Obregón (1996) (i.e. 0.345 and 0.522 versus 0.999, as seen in rows 3, 4, and 2 of Fig. 4), the one based on 4 interpolating points is the best, at least by a factor of two, in regards to deviations on lag-one derivatives ( $\sum \Delta^d$ ) (i.e. 0.643 versus 1.509, as reported in rows 5 and 4, respectively). These sets, that nicely capture not only the texture of the records but also the noticeably dominant major peak, hence provide better overall results than those presented in Puente and Obregón (1996). These derived measures, especially the ones resulting from 5 points, possess indeed the right amount of roughness (better than the previous best, especially from the beginning of the event to the major peak), as reflected by the closeness in the three attributes  $S$ ,  $L$ , and  $R$  and the lower values of the quantity  $D$ , for both levels of aggregation. Notice that this happens despite the fact that their FM parameters are rather different (see Table 1), as reflected by the fractal dimension of the graphs of their interpolating functions of 1.42, 1.29, and 1.26 for, in order,  $dy^*V$  WRR96,  $dy^*V$ , and  $dy^*IV$ .

In order to illustrate the goodness of the approximations just presented, Figs. 5 and 6 include other statistical information not used explicitly in the optimization search. In consonance with the results presented in Puente and Obregón (1996), Fig. 5 presents the marginal distribution of the rainfall records (i.e. its histogram), and a summary of relevant moments, i.e. central moments in time (Cm), modal moments in time (Mm), and central moments from the rainfall intensity axis (Cms), with percentages indicating deviations of the model results with respect

to the actual data, and Fig. 6 includes the autocorrelation functions, power spectra and multifractal spectra, for all sets in the right hand side of Fig. 4.

As readily appreciated from Fig. 5, the performance on all of these attributes (with historical histograms shown in white) confirms that the ‘optimized storms’ emanating from 4 and 5 points are the best, particularly the latter. Curiously, but understandably, given the improved search procedure, the new storms, particularly those obtained via 5 interpolating points, are found better in regards to Cm, Mm and Cms than the one presented earlier by Puente and Obregón (1996), that explicitly optimized such attributes. As seen, while both FM storms corresponding to 5 interpolating points give similar fits on the marginal distribution and also provide similar error values for all the moments of orders 1 and 2, the FM storm corresponding to 4 points yields a histogram biased towards small rainfall values (see Fig. 4, right,  $dy^*IV$ ) and, hence, gives larger errors in the variance of the records as seen from the rainfall intensity axis (Cms).

As seen in Fig. 6 (with historical information in white), the trends just mentioned are maintained also while considering autocorrelation functions, power spectra and multifractal spectra (especially the left portion of this attribute). The two storms based on fractal functions passing by 5 interpolating points and the one based on 4 points give indeed fairly accurate approximations for these attributes, as further visualized by the close agreement in the correlation lengths defined from a decay of  $e^{-1}$ ,  $\tau(e^{-1})$ , and the length to the first local minimum,  $\tau(\text{flm})$ , the power spectrum scaling exponent,  $\beta$ , and the multifractal spectrum’s entropy dimension,  $D_1$ .

As the agreement in all attributes for the FM sets related to 4 and 5 interpolating points is certainly reasonable, one may safely infer that the FM approach does produce measures that preserve the most important statistics of the Boston storm, while providing a parsimonious representation of the whole set of records. The fact that this is accomplished with only 14 parameters for the case based on 5 interpolating points, leading to a ‘compression’ ratio of  $1990/14 \approx 142$ , is certainly encouraging. This is particularly the case, as the geometric approach captures even small fluctuations, truly present or not.

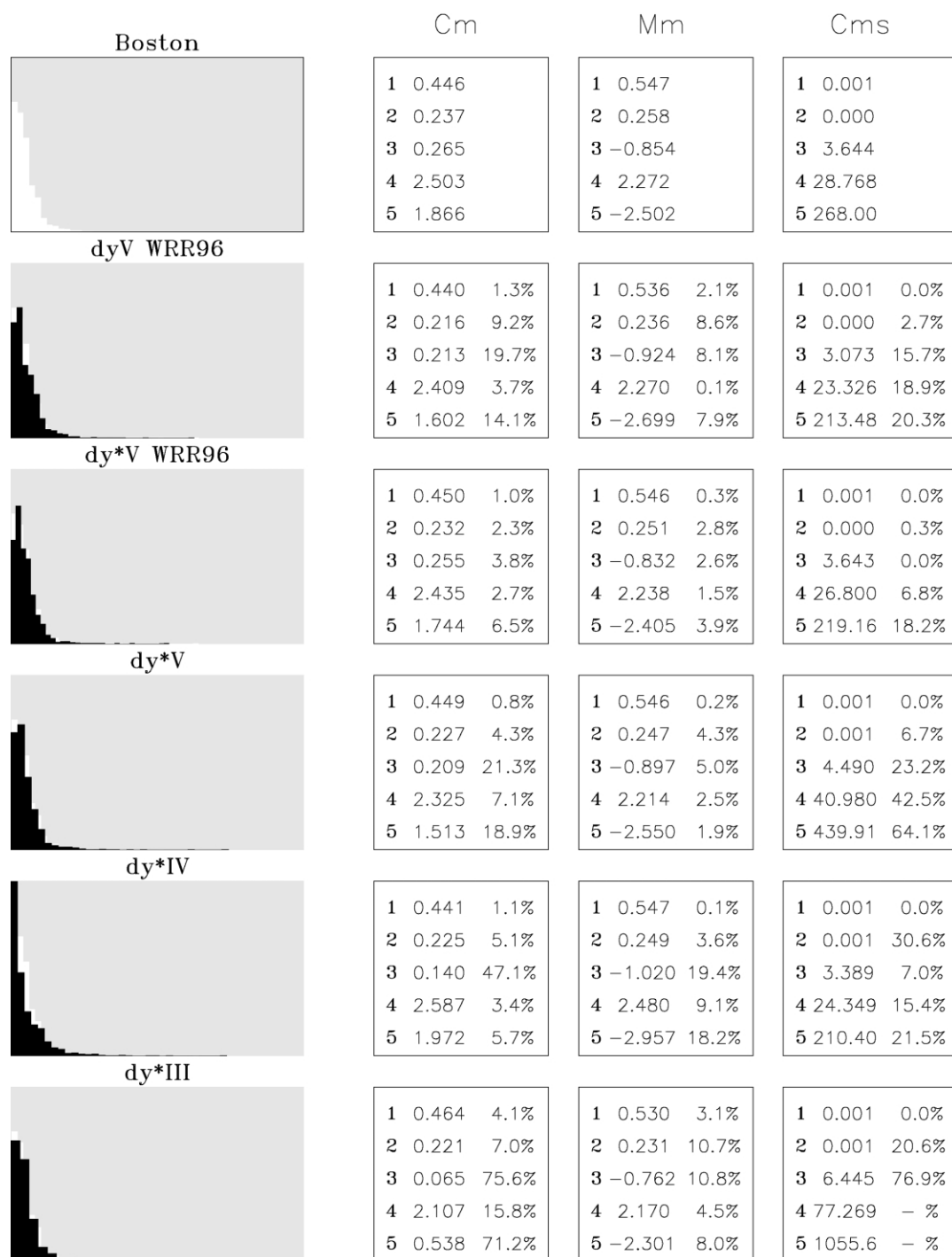


Fig. 5. Histogram, central (Cm) and modal (Mm) moments in time, and central moments in the intensity axis (Cms) for the storms in Fig. 4 having 1990 points. Percentages indicate deviations of model results with respect to the actual data. All histograms have as horizontal and vertical scales [0, 0.01] and [0, 188], respectively.

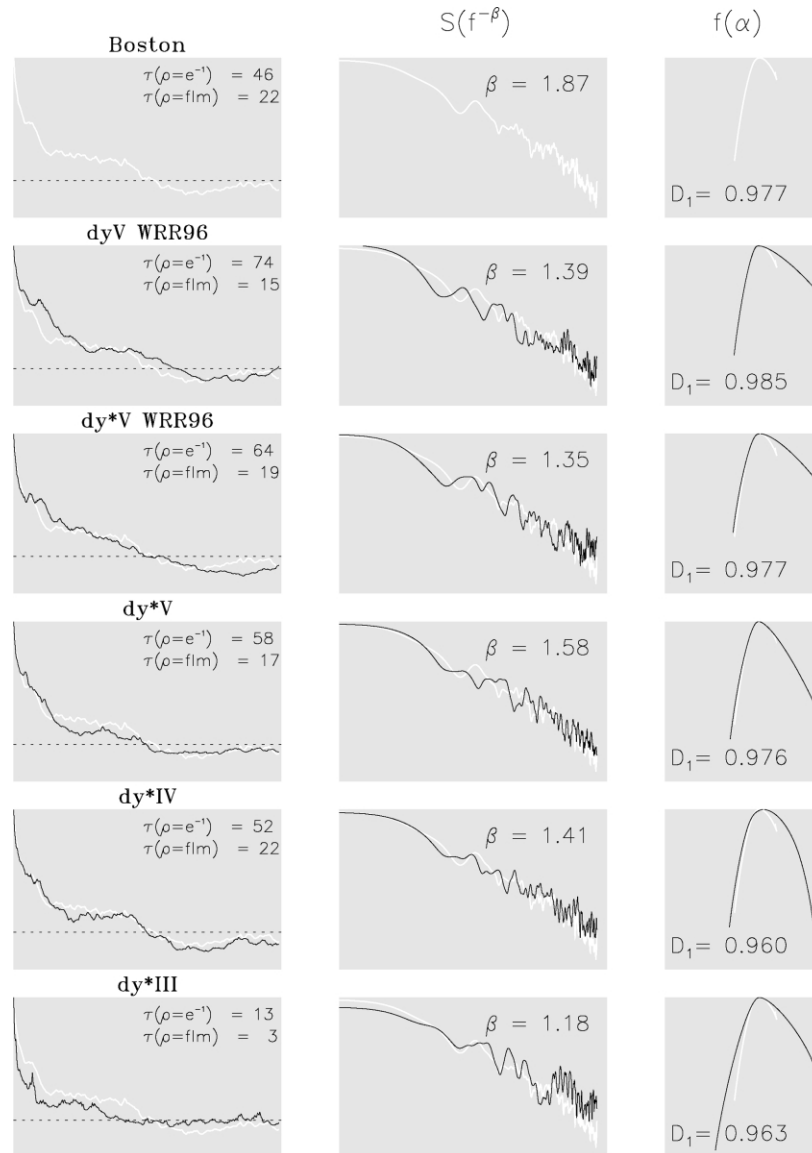


Fig. 6. Autocorrelation function, power spectrum and multifractal spectrum for the storms in Fig. 4 having 1990 points. These functions have as horizontal and vertical scales, in order,  $[0, 500]$  and  $[-0.3, 1]$ ,  $[0.005, 4]$  and  $[0.001, 25]$  in log–log scale, and  $[0, 1.75]$  and  $[0, 1]$ .

#### 4. Conclusions

The present study followed the research undertaken by Puente and Obregón (1996), who reported usage of a deterministic FM procedure to encode a storm event in Boston as the derived distribution of a multinomial multifractal measure via a fractal interpolating function. In an attempt to study if better FM

representations may be obtained for such an event, this study presented a detailed sensitivity analysis that encompassed: (a) using two distinct objective functions based on cumulative distributions of the records and their lag-one derivatives; (b) performing the parameter estimation search via a genetic algorithm; (c) using fractal interpolating functions passing by 3, 4, and 5 points while considering all possible sign

combinations of the scaling parameters of the FM affine mappings; and (d) employing the Boston records at two different levels of aggregation.

While the study revealed that better FM approximations, based on fractal functions passing by 4 and 5 interpolating points and corresponding to 10 and 14 parameters having markedly distinct parameter values, could indeed be obtained to improve the previous fit for the Boston storm, it also showed that it is unescapable to do the analysis at the records' resolution, for good FM approximations of the aggregated data often translate into unseen intermittencies at the data's scale. Despite the improvements, these results suggest that further work is needed so that the FM method may perform even better. Amongst the subjects that should be studied there are: (a) the proper design of an objective function for the FM search, (b) the appropriate definition of an efficient (genetic) algorithm for the inverse problem, i.e. with suitably defined probabilities, and (c) the consideration of extensions of the FM methodology so that other interpolating functions and parent measures are employed.

As has been illustrated, the results herein confirm that FM representation may be used to simulate the overall geometric appearance of complex rainfall records in a whole and deterministic fashion, via an algorithm that turns out to be structurally rather simple. Successful usage of the ideas to other rainfall records gathered in Iowa City has been accomplished and its results are reported elsewhere (Obregón et al., 2002).

The results from these studies and others do suggest that the FM approach may be used as a tool for the synthetic generation of rainfall sets and do indicate that such a procedure (or its extensions) may eventually be used, in light of their inherent compression of information, as parsimonious means for archiving data. It is envisioned that relevant physics may be extracted via the FM representation, for its parameters, by reflecting the intrinsic geometry, may be used to discriminate alternative sets under different climatic and geographic conditions.

## Acknowledgements

The work presented in this article was supported in part by the USEPA via Grant GAD

# R824780 and by NASA under Grant NAG5-7441.

## References

- Barnsley, M.F., 1988. *Fractals Everywhere*, Academic Press, San Diego, CA.
- Berndtsson, R., Jinno, K., Kawamura, A., Olsson, J., Xu, S., 1994. Dynamical systems theory applied to long-term temperature and precipitation time series. *Trends Hydrol.* 1, 291–297.
- Duan, Q., Sorooshian, S., Gupta, V., 1992. Effective and efficient global optimization for conceptual rainfall–runoff models. *Water Resour. Res.* 28 (4), 1015–1031.
- Feder, J., 1988. *Fractals*, Plenum Press, New York.
- Lorenz, E.N., 1963. Deterministic nonperiodic flow. *J. Atmos. Sci.* 20, 130–141.
- Lovejoy, S., Schertzer, D., 1990. Multifractals, universality classes and satellite and radar measurements of cloud and rain fields. *J. Geophys. Res.* 95, 2021–2034.
- Meneveau, C., Sreenivasan, K.R., 1987. Simple multifractal cascade model for fully developed turbulence. *Phys. Rev. Lett.* 59, 1424–1427.
- Obregón, N., Puente, C.E., Sivakumar, B., 2002. Modeling high resolution rain rates via a deterministic fractal–multifractal approach. *Fractals* 10 (3), 387–394.
- Otten, R.H.J.M., van Ginneken, L.P.P.P., 1989. *The Annealing Algorithm*, Kluwer Academic, Norwell, MA.
- Press, W.H., Flannery, B.P., Teukolsky, S.A., Vetterling, W.T., 1989. *Numerical Recipes*, Cambridge University Press, New York.
- Puente, C.E., 1992. Multinomial multifractals, fractal interpolators, and the Gaussian distribution. *Phys. Lett. A* 161, 441–447.
- Puente, C.E., 1994. Deterministic fractal geometry and probability. *Int. J. Bifurcations Chaos* 4 (6), 1613–1629.
- Puente, C.E., Obregón, N., 1996. A deterministic geometric representation of temporal rainfall: results for a storm in Boston. *Water Resour. Res.* 32 (9), 2825–2839.
- Rodríguez-Iturbe, I., De Power, F.B., Sharifi, M.B., Georgakakos, K.P., 1989. Chaos in rainfall. *Water Resour. Res.* 25 (7), 1667–1675.
- Sivakumar, B., Liong, S.Y., Liaw, C.Y., Phoon, K.K., 1999. Singapore rainfall behavior: chaotic? *J. Hydrol. Engng.* ASCE 4 (1), 38–48.
- Sivakumar, B., Sorooshian, S., Gupta, H.V., Gao, X., 2001. A chaotic approach to rainfall disaggregation. *Water Resour. Res.* 37 (1), 61–72.
- Sreenivasan, K.R., 1991. Fractals and multifractals in fluid turbulence. *Annu. Rev. Fluid Mech.* 23, 539–600.
- Tessier, Y., Lovejoy, S., Schertzer, D., 1993. Universal multifractals: theory and observations for rain and clouds. *J. Appl. Meteorol.* 2, 223–250.
- Zhou, J.L., Tits, A.L., 1993. Nonmonotone line search for minimax problems. *J. Opt. Theory Appl.* 76, 455–476.